Journal Pre-proof

Fracture network analysis of Yacoraite Formation in the Tres Cruces sub-basin, northwestern Argentina

Clara Correa Luna, Daniel L. Yagupsky, Jeremías Likerman

PII: S0895-9811(19)30362-1

DOI: https://doi.org/10.1016/j.jsames.2019.102446

Reference: SAMES 102446

To appear in: *Journal of South American Earth Sciences*

Received Date: 15 July 2019

Revised Date: 29 November 2019

Accepted Date: 29 November 2019

Please cite this article as: Luna, C.C., Yagupsky, D.L., Likerman, Jeremí., Fracture network analysis of Yacoraite Formation in the Tres Cruces sub-basin, northwestern Argentina, *Journal of South American Earth Sciences* (2020), doi: https://doi.org/10.1016/j.jsames.2019.102446.

Fracture network analysis of Yacoraite Formation in the Tres Cruces sub-basin, northwestern Argentina

Clara Correa Luna [a, *], Daniel L. Yagupsky [a, b], Jeremías Likerman [a, b]

[a] Instituto de Estudios Andinos Don Pablo Groeber (IDEAN), CONICET – Universidad de Buenos Aires. Buenos Aires, Argentina
[b] Universidad de Buenos Aires. Facultad de Ciencias Exactas y Naturales. Departamento de Ciencias Geológicas. Buenos Aires. Argentina
[*] Corresponding autor. Tel.: +54 11 4576 3400. E-mail addresses: claracorrealu@gmail.com, clara@gl.fcen.uba.ar (C. Correa Luna)

Keywords
Fracture network; joints; fold; Yacoraite Formation; Tres Cruces sub-basin

Abstract

The Tres Cruces sub-basin, located in Jujuy province, northwestern Argentina, is characterized by intense N-S folding and faulting. These structures were formed as a result of the Cenozoic shortening that produced the tectonic inversion of the Salta Rift Basin normal faults. Some of the main folds and faults show abrupt trend variations, controlled by NW-SE transverse lineaments. We performed a fracture network analysis over the Maastrichtian-Danian limestones of the Yacoraite Formation, at three folds located in the central sector of the sub-basin. A total of 832 planar fractures were measured in different structural domains. Five main fracture sets were identified, trending NW-SE, NE-SW, ENE-WSW, WNW-ESE and N-S to NNW-SSE. Their relative chronology was established based on the observed abutting relationships. The analysis performed suggests that NW-SE, NE-SW and ENE-WSW trending sets are regionally represented and were formed before the initial stages of folding. Set ENE-WSW is sub-parallel to the convergence direction acting during the Neogene. The other two sets are associated with local perturbations of the far-field signal control by the oblique NW-SE lineaments. The origin of the WNW-ESE set remains unclear; its distribution is locally restricted to the San Bernardo domain. Finally, the N-S to NNW-SSE set shows a synfolding origin generated when the surveyed folds were growing. We then place the various identified fracture sets into a single stress field setting, perturbed by the leading NW-SE transverse lineaments that dominate this region.

1. Introduction

In the past years, the oil industry has shown an increasing interest in fractured reservoirs (e.g. Engelder et al., 2009; Hardebol et al., 2015; Casini et al., 2016; Panza et al., 2016). Likewise, the characterization of fractures and fracture networks contribute to a deeper understanding of rock deformation. Extensive research has been conducted to examine the relationship between fracture generation and larger structures, such as faults and folds (e.g. Stearns and Friedman, 1972; Twiss and Moores, 1973; Hancock, 1985; Nelson, 2001; Bellahsen et al., 2006; Tavani et al. 2006). However, there is much less information about the effects of preexisting anisotropies on the over-imposed fracture patterns (e.g. Bergbauer and Pollard, 2004; Tavani et al., 2015), and the result of stress field perturbations around pre-existing faults (Rawnsley et al., 1992; Homberg et al., 1997; Homberg et al., 2004; Maerten et al., 2016; Maerten et al., 2018).

The Yacoraite Formation limestones, in northwestern Argentina, constitute a well-known case study of a naturally fractured reservoir (Hernández et al., 1999; Starck, 2011; Grosso et al., 2013). It is characterized by a calcareous-dolomitic composition and represents the early post-rift stage of the Cretaceous to Paleogene Salta Group in the Salta Rift Basin (Mon and Salfity, 1995; Disalvo et al., 2002; Marquillas et al., 2005). Few previous studies have reported fracture patterns in the Yacoraite Formation (e.g. Grosso et al., 2013; Hernández et al., 2016; Hernández and Franzese, 2017), and none of them has been made in the Tres Cruces sub-basin. In this paper, we present and discuss the outcropping fracture patterns of the Yacoraite Formation at three different folded structures located in the Tres Cruces sub-basin: the San Bernardo Syncline, the Arroyo Cóndor folds, and the Tres Cruces Eastern Anticline. Here we propose an evolutionary model for the fracture record and its relationship with the folding and the tectonic stresses acting in the area through the Cenozoic, intending to assess the role of stress perturbation due to pre-existing faults and structural weaknesses.

Our work explains de recognized fracture pattern considering a single-stage stress far-field that can be locally controlled by the presence of preexisting structural anisotropies in the basement. Assessment of these controlling factors on fracturing is thus of importance to the characterization of fractured reservoirs.

2. Geological Setting

The study area is located in the northern Eastern Cordillera between the Puna plateau to the west and the Subandean Ranges to the east (Fig. 1.a). It constitutes a bivergent thick-skinned fold and thrust belt with prevailing N-S trends (Gangui, 1998, Kley et al., 2005, Hongn et al., 2007; Monaldi et al., 2008b). The structural style is dominated by inversion of the Cretaceous extensional faults of the Salta Rift Basin during Cenozoic times (Grier et al., 1991; Mon and Salfity, 1995; Kley et al., 2005; Carrera et al., 2006; Carrera and Muñoz, 2008; Monaldi et al., 2008a).

2.1. Tectonic setting

The Central Andes were formed as a consequence of the convergence between the oceanic Nazca Plate and the continental South American Plate (e.g. Allmendinger et al., 1997; Pardo-Casas and Molnar, 1987; Somoza and Ghidella, 2012). Although some controversy persists regarding the beginning of the formation of the Andean foreland basin, several studies suggest that deformation has been propagating eastward in pulses since at least the middle Eocene (e.g. Salfity and Marquillas, 1994; Oncken et al., 2006; Hongn et al., 2007; Payrola et al., 2009; Montero-López et al., 2018).

The Eocene contractional phase is widely recognized in the Puna/southern Altiplano, the Eastern and Western Cordilleras, where it represents the first stage of Andean shortening (Coutand et al., 2001; del Papa et al., 2004; Elger et al., 2005; Hongn et al., 2007; Oncken et al., 2006; Payrola et al., 2009; Montero-López et al., 2018). The principal event involving shortening and uplift in Central Andes occurred during the Miocene (Oncken et al., 2006; Payrola et al., 2009). This event gave rise to the tectonic inversion of the Salta Rift Basin's normal faults generated in the Early Cretaceous (Salfity and Marquillas, 1994; Rubiolo et al., 2001). Finally, deformation shifted to the east forming the Subandean fold and thrust belt from Pliocene to present (Coutand et al., 2001; Oncken et al., 2006).

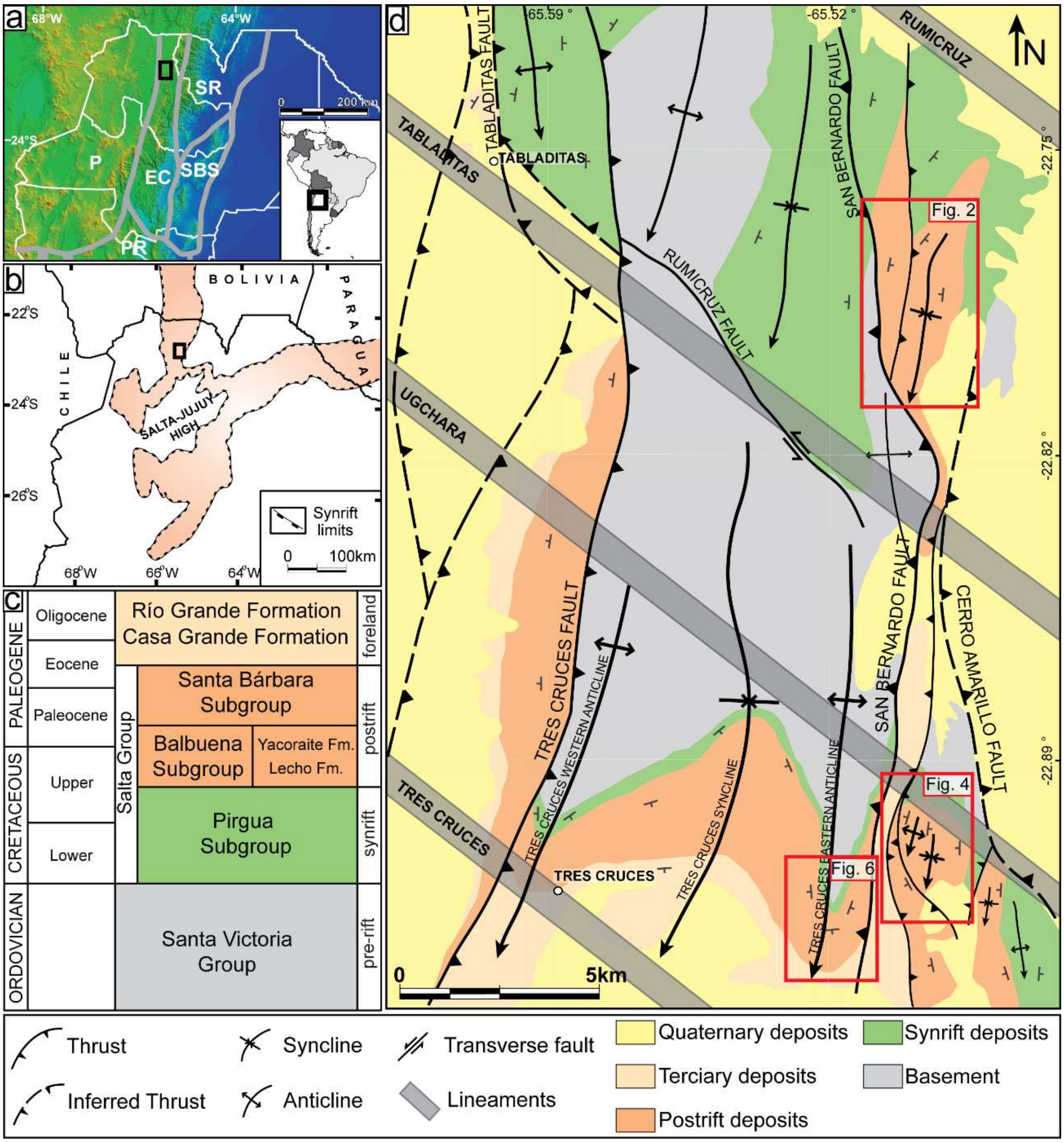

Fig. 1. a) Geological provinces of northwestern Argentina (P: Puna; EC: Eastern Cordillera; SR: Subandean Ranges; SBS: Santa Barbara System; PR: Pampean Ranges). b) Map of the Salta Rift Basin showing the synrift limits adapted from Marquillas et al. (2005); black rectangles in a and b show the study area location. c) Stratigraphic chart of the study area. d) Geological map of the study area showing the main structures and units, modified from Boll and Hernandez (1986) and Gangui and Götze (1996). Red squares indicate the three work areas: San Bernardo (Fig. 2), Arroyo Cóndor (Fig. 4) and Eastern Tres Cruces (Fig. 6).

Paleomagnetic data show a NE-SW convergence direction between Eocene to Oligocene times that changes to ENE-WSW from Neogene to recent times (Pardo-Casas and Molnar, 1987; Somoza and Ghidella, 2012). In turn, available fault-kinematic analyses reveal an E-W shortening direction for the Miocene near Abra Pampa, west of the study area (Cladouhos et al., 1994).

2.2. Stratigraphy

The oldest rocks exposed in the study area are the Ordovician marine shales of the Santa Victoria Group (Salfity and Marquillas, 2000) (Fig. 1.c). During the Early Cretaceous, an extensional phase took place in the area generating isolated depocenters that radiate from a central positive block: the Salta-Jujuy High (Fig. 1.b). These depocenters got interconnected during the Upper Cretaceous, developing the Salta Rift Basin (Mon and Salfity, 1995). The Salta Group is the rift-related sequence that overlies the Ordovician deposits and is subdivided into three subgroups: Pirgua, Balbuena and Santa Bárbara (Fig. 1.c) (e.g. Marquillas et al., 2005).

The Pirgua Subgroup consists of red continental sandstones and conglomerates, with volcanic and volcaniclastic intercalations; it is interpreted as the Early to Late Cretaceous synrift (Reyes and Salfity, 1973; Marquillas et al., 2005). Early post-rift units are represented by the Balbuena Subgroup that overlays the synrift deposits, connecting the depocenters with lacustrine to restricted marine carbonates and evaporitic deposits. These rocks reflect the Late Cretaceous Atlantic ingression, represented by the Yacoraite Formation (Mon and Salfity, 1995; Marquillas et al., 2005). The Santa Bárbara Subgroup conforms the late post-rift stage of the basin. It is formed by red fine-grained sandstone and green mudstone (Moreno, 1970; Marquillas et al., 2005). As a result of the Andean contraction during the Cenozoic, tectonic inversion of normal faults (Grier et al., 1991; Mon and Salfity, 1995; Carrera et al., 2006) led to the development of a foreland basin infilled with Tertiary (Eocene to Oligocene) fluvial synorogenic deposits of Casa Grande and Río Grande formations (Fig. 1.c) (Boll and Hernandez, 1986; Bond and Lopez, 1995; González et al., 2004).

2.3. Structure

The Tres Cruces sub-basin is the northernmost depocenter of the Salta Rift Basin (Fig. 1.b). Its orientation is N-S and continues into Bolivia to the north forming the Andean Basin (Reyes, 1972). This sub-basin is characterized by the presence of intense N-S trend folding and faulting that show along-strike variations controlled by NW-SE to WNW-ESE regional transverse lineaments (Fig. 1.d). These lineaments are interpreted as pre-Cretaceous basement heterogeneities, reactivated during the Cretaceous extensional phase and the Andean structuration, compartmentalizing the deformation (Boll and Hernández, 1986; Kley et al., 2005; Monaldi et al., 2008a). In the analyzed area, both Tabladitas and San Bernardo thrusts are controlled by the Tabladitas Lineament, turning its trends from N-S to NW-SE (Fig. 1.d). Moreover, in the Tabladitas area, synrift outcrops observed north of the lineament disappear to the south, and in the central area, folds are interrupted towards this lineament. Ugchara Lineament acts as a discontinuity limiting the development of the Cerro Amarillo Thrust and folds in the Arroyo Cóndor area (Fig. 1.d). Synrift thickness variations and changes in thrusts vergence across the transverse lineaments have been also informed by Boll and Hernández (1986). Therefore, it might be inferred that these lineaments acted as transfer zones during the Andean structuration of the area.

The study area is located within the central sector of the Tres Cruces sub-basin, bounded to the east by the west-vergent Cerro Amarillo Fault (Fig. 1.b and d). Two important thrusts with opposite vergences were recognized: the west-vergent Tres Cruces Fault and the east-vergent San Bernardo Fault. Between them, two south-plunging anticlines cored by Lower Paleozoic strata appear, forming the south-plunging Tres Cruces Anticlinorium with a general N-S trend (Fig. 1.d). A system of four sub-parallel, transverse lineaments were mapped in the area: Tres Cruces, Ugchara, Tabladitas and Rumicruz (Fig. 1.d). As mentioned earlier, they interrupt, deviate and/or change the vergence of some of the main N-S thrusts and folds. Fractures were measured over folds affecting the Yacoraite Formation limestones along three working areas: San Bernardo, Arroyo Cóndor and Eastern Tres Cruces (Fig. 1.d).

The San Bernardo area (Figs. 1.d and 2) is dominated by the San Bernardo Syncline, bounded by two NW-SE lineaments: Tabladitas to the south and Rumicruz to the north. The San Bernardo south-plunging syncline presents an approximate N-S orientation and shows an abrupt change to NE-SW at its northern termination (Fig. 1.d). It is located in the hanging wall of the N-S west-vergent thrust that repeats post-rift deposits of Balbuena Subgroup. To the west, a regional east-vergent N-S thrust uplifts a basement block (Santa Victoria Group) on top of early post-rift deposits, adopting a NW-SE trend near the Tabladitas lineament (Fig. 1.d).

In the Arroyo Cóndor area (Figs. 1.d and 4) fracture measurements were performed along two south-plunging folds with N-S to NNE-SSW orientation, named here Central Anticline and Central Syncline. These folds are in the footwall of an east-vergent thrust with NNE-SSW orientation in the north of the mapped area, turning to NW-SE to the south (Fig. 1.d). They are limited to the north by the NW-SE Ugchara lineament.

In the Eastern Tres Cruces area (Figs. 1.d and 6), fractures were measured over the N-S trending Tres Cruces Eastern Anticline (Fig. 1.d). This fold plunges to the south, forming part of the Tres Cruces Anticlinorium. It is located in the hanging wall of the east-vergent NNE-SSW trending San Bernardo reverse fault. This structure exposes basement and syn-rift units and uplifts post-rift deposits of Balbuena Subgroup on top of Tertiary synorogenic deposits (Figs. 1.d and 6).

3. Methodology

3.1. Data Collection

The Yacoraite Formation limestones present well-exposed outcrops in the area, showing an intense fracture network. These fractures are well developed in the northern part of the Tres Cruces sub-basin. A total of 832 fractures were measured from three working areas (San Bernardo, Arroyo Cóndor and Eastern Tres Cruces; Fig. 1.d). In each area, measurements were made when possible at different structural domains of the folds (e.g. forelimb, backlimb, hinge zone and fold termination). Also, schematic cross-sections were performed based on field data and 2D seismic sections (Figs. 2, 4 and 6), not shown for confidentiality reasons. Their orientations were chosen in other to extrapolate the structures identified in the seismic lines as parallel as possible to their strikes.

Most of the measured fractures were classified as tensile joints, mode I (Engelder, 1987; Pollard and Aydin, 1988), since they present opening displacement and contain a coarse calcite mineral filling, that is indicative of opening mode fractures (Bellahsen et al., 2006). Plumose structures, i.e., common and characteristic features of mode I fractures (Engelder, 1987; Pollard and Aydin, 1988), are sometimes preserved on their surfaces. When evidence of tail cracks or Riedel fractures were observed in the field, fractures were classified as shear fractures, mode II. However, in some cases deformation mode is difficult to determine, given the absence of positive evidence of shear, opening displacements or mineral fills, features only occasionally preserve in outcrop. Upon the absence of positive evidence of fracture mode, features observed on other fractures with similar orientation were considered to characterize the deformation mode. The dominant occurrence of mode I joints and veins allows the use of the resulting fracture sets as indicators of orientations of paleo-σ3 trends (Engelder, 1987) and compared them with regional stress directions as will be discussed later.

Fractures orientation, spacing, and deformation mode (when possible) were systematically surveyed using linear and circular scanlines. Linear scanlines are 1-dimensional lines of observation where fractures that intersect the selected line are measured (Priest and Hudson, 1981). The orientation of this type of scanline is chosen to represent better fracture sets. Although this method allows many measurements in short time, collected data is still subject to orientation censoring and length biases. Circular scanlines eliminate most sampling biases caused by scanline orientations and also correct errors due to censoring and length bias (Mauldon et al., 2001; Rohrbaugh et al., 2002).

Finally, the relative chronology of fracture sets was inferred from abutting relationships among fractures, considering that younger fractures abut against older ones (Hancock, 1985; Peacock and Sanderson, 2018). Reliable fracture chronology was considered when abutment relationships were consistent and repetitive between sets. In addition, cross-jointed ‘ladder-like’ fracture patterns resulting from a single deformational event was evaluated, considering if cross joint occurs between a selective spacing of joint pairs.

3.2. Data processing

For each site, fracture data is presented in an equal-area projection on the lower hemisphere, with density contours representing fracture data and great circles representing the mean plane of each fracture set using Stereonet program (Allmendinger et al., 2012; Cardozo and Allmendinger, 2013).

Common orientation can be identified only after backtilting the data along the bedding strike to their attitude prior to the folding. To unfold the data, the following assumptions are considered. First, although abrupt strike modifications of structures are observed, it is assumed that the sites would not have undergone significant rotation about a vertical axis since these modifications are associated with transfer zones. Second, the local fold axes are considered subhorizontal, given their low axial plunge values. Commonality of fracture orientation, after removal of bedding dip, is taken as supportive of a pre-folding origin, where the fractures are subparallel and bed perpendicular (Hancock, 1985). However, fracture orientations parallel or perpendicular to bedding strike are not affected by bedding unfolding and may be interpreted as occurring during any stage of fold growth (Lacombe et al., 2011). Under efficient flexural slip, some bedding-perpendicular tensile joints can develop at the onset of folding, becoming superimposed on true pre-folding structures. In this way, the two principal stress axes can remain parallel to the bedding (Tavani et al., 2006; Lacombe et al., 2011). In order to prevent this as a source of misinterpretation, on hinge zone stations, orientation clustering was prioritized over their bed perpendicular attitude to determine the relative chronology between fractures and folding.

	Set NW-SE				Set NE-SW				Set N-S				Set ENE-WSW				Set WNW-ESE			
	N	Strike/Dip	α95	K	N	Strike/Dip	α95	K	N	Strike/Dip	α95	K	N	Strike/Dip	α95	K	N	Strike/Dip	α95	K
San Bernardo area																				
Site 1	47	327/82	3	50	--	--	--	--	20	004/80	5	6	45	265/84	4	36	97	296/84	2	48
Site 2	8	300/90	0	5,79E+15	13	020/86	4	93	10	172/90	3	199	--	--	--	--	--	--	--	--
Site 3	--	--	--	--	--	--	--	--	39	166/78	2	135	17	247/87	3	141	--	--	--	--
Arroyo Cóndor area																				
Site 4	22	130/63	10	10	7	215/83	14	16	--	--	--	--	33	075/80	5	24	--	--	--	--
Site 5	--	--	--	--	81	204/84	3	31	--	--	--	--	9	067/72	11	22	--	--	--	--
Site 6	29	314/78	7	14	8	039/86	6	82	8	354/82	10	31	--	--	--	--	11	284/87	3	291
Site 7	--	--	--	--	78	033/82	5	10	--	--	--	--	--	--	--	--	--	--	--	--
Eastern Tres Cruces area																				
Site 8	--	--	--	--	18	031/83	5	45	25	353/85	4	48	12	076/83	7	36	--	--	--	--
Site 9	--	--	--	--	--	--	--		18	170/82	8	20	25	082/89	5	33	--	--	--	--
Site 10	6	315/82	7	84	20	223/90	4	89	5	179/89	4	333	6	265/74	7	83	--	--	--	--

Table 1. Table of fracture set data (headings) showing the number of fractures (N), Fisher Strike/Dip results using right-hand rule, α95% confidence angle and K parameter of the sets for each sampling site calculated after the rotation.

Different fracture sets were identified based on data clustering after bed dip removal. The Fisher mean fracture plane was calculated for each set along with the α95% confidence angle and the K parameter to evaluate the set confidence (Fisher et al., 1987) (Table 1).

4. Results

4.1. San Bernardo area

A total of 336 fractures were measured in three selected sampling sites along the San Bernardo Syncline. Site 1 is situated to the south of the western flank of the fold, near the inflection from N-S to NW-SE strike of the San Bernardo Fault. This site was chosen due to the outcrop quality and the proximity to the fault inflection. Sites 2 and 3 are both located in the eastern flank. Site 3 is almost at the same latitude as Site 1, and Site 2 is approximately 1 km to the north (Fig. 2). Five main fracture sets are recognized.

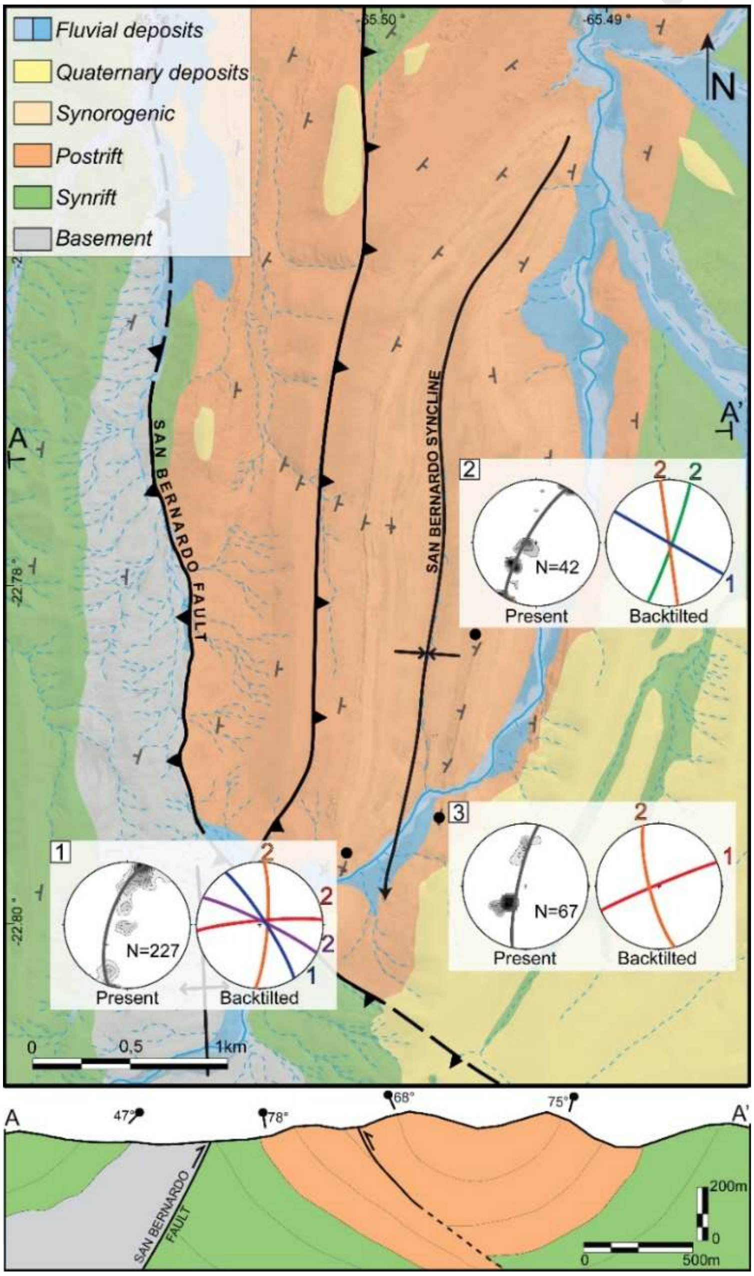

Fig. 2. Top: geological map of the San Bernardo area (see Fig. 1 for structural references and location); black numbered dots indicate sampling sites. Equal-area plots show (left) present-day density contour of poles to planes and bed attitude (grey great circle), and (right) great circles for Fisher mean fracture set orientations

in backtilted position. Numbers indicate the relative chronology observed, being 1 the oldest. Bottom: schematic cross-section, based on field data (see location on map).

Most of the fractures measured in this area are sub-vertical tensile joints. The longest fractures exceed the diameter of the circular scanlines (2 meters) and they are roughly NW-SE. ENE-WSW and WNW-ESE sets present the largest number of fractures in site 1, with trace lengths ranging from 10 to 50 cm. Fractures belonging to the N-S to NNW-SSE trending set are subparallel to the fold axis. Finally, a minor fracture set with NE-SW to NNE-SSW orientation is recognized in site 2 (Fig. 2). Fractures belonging to N-S and NE-SW sets are shorter than those from NW-SE set, and their lengths range from 10 to 70 cm (Fig. 3.b and d).

Abutting relationships indicate that the NW-SE set is the oldest, while the relative chronology between the other four sets remains unclear given the ambiguity observed in their terminations (Fig. 3).

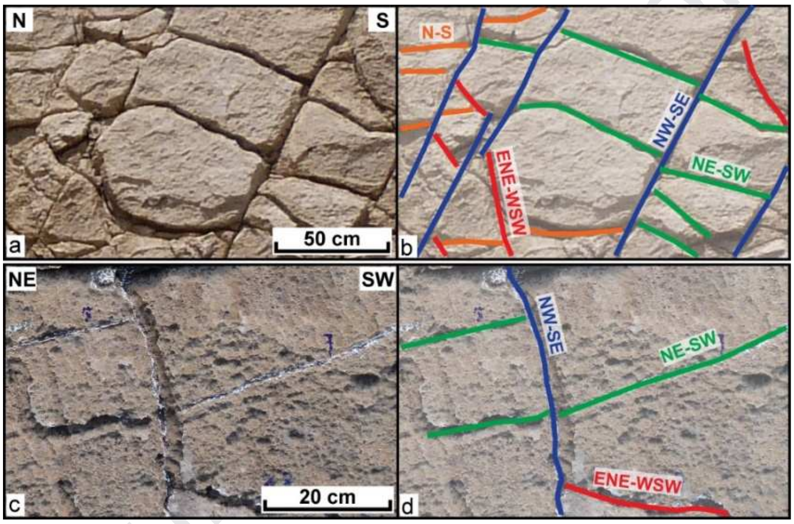

Fig. 3. Outcrop photographs and interpretation near site 3 (a and b) and in site 2 (c and d) showing examples of fracture patterns in the San Bernardo area (see Fig. 2 for location).

4.2. Arroyo Cóndor area

A total of 344 fractures were measured in this area. Sampling sites were distributed through the Central Anticline and the Central Syncline (Fig. 4). Sites 4 and 6 are located on the western and eastern flank of the anticline respectively, and site 5 on its hinge zone. Finally, site 7 is on the eastern flank of the syncline (Fig. 4).

Five tensile fracture sets are identified in the area. The most representative one presents NE-SW to NNE-SSW orientations and includes sub-vertical fractures of highly variable trace lengths, ranging from more than 2 meters to 20 centimeters (Fig. 5.b and d). Similar amounts of fracture were measured for fracture sets trending NW-SE and ENE-WSW with lengths of 50-60 cm and 20-30 cm respectively. Finally, there are two minor sets of sub-vertical fractures with N-S and WNW-ESE mean strikes.

Abutting relationships are ambiguous comparing the different sites. In site 4, NW-SE set was developed first, because ENE-WSW and NE-SW fractures abut against it (Fig. 5.a and b). However, in site 6, NW-SE set mostly abuts NE-SW set, suggesting that the former may be younger (Fig. 5.c and d).

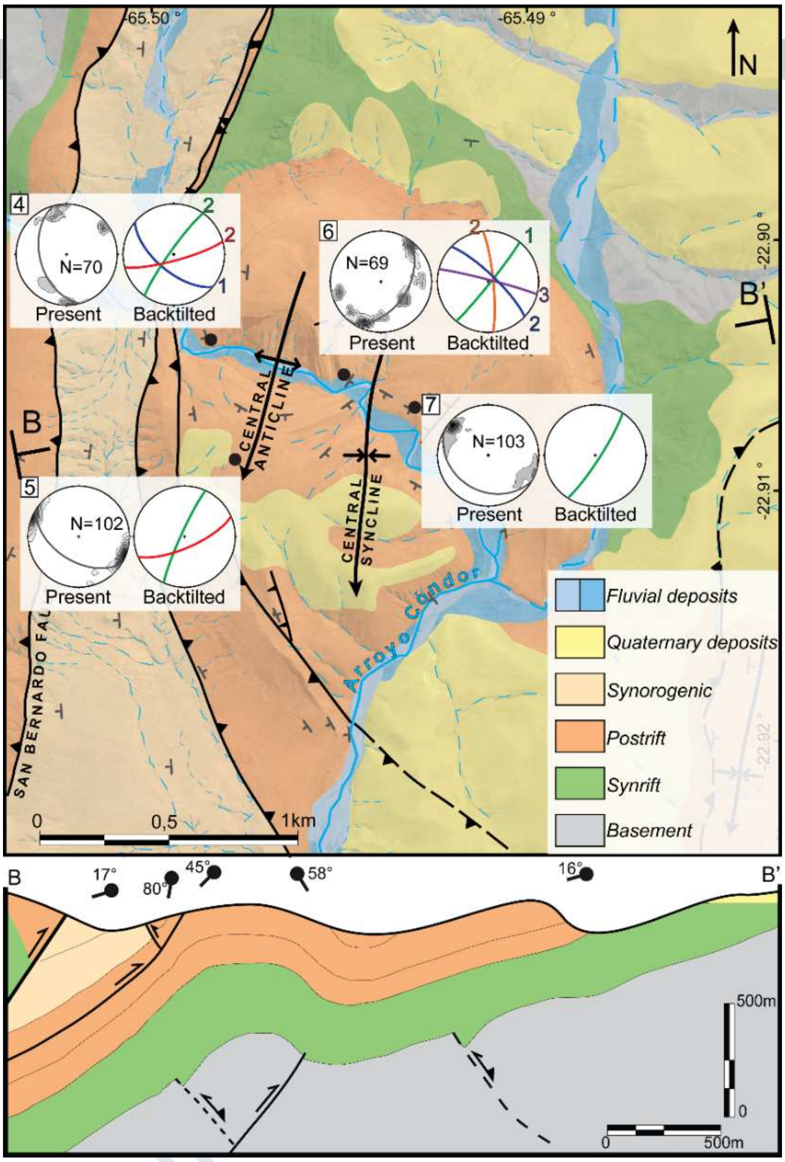

Fig. 4. Top: geological map of the Arroyo Cóndor area (see Fig. 1 for structural references and location); black numbered dots indicate sampling sites. Equal-area plots show (left) present-day density contour of poles to planes and bed attitude (grey great circle), and (right) great circles for Fisher mean fracture set orientations in backtilted position. Numbers indicate the relative chronology observed, being 1 the oldest. Bottom: schematic cross-section, based on field data and proprietary 2D seismic lines (see location on map).

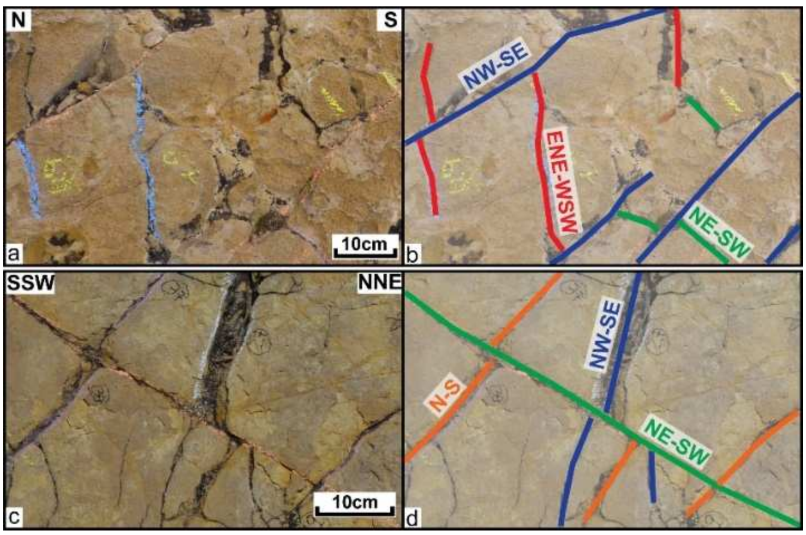

Fig. 5. Outcrop photographs and interpretation in site 4 (a and b) and in site 6 (c and d) showing examples of fracture patterns in the Arroyo Cóndor area (see Fig. 4 for location).

4.3. Eastern Tres Cruces

152 fractures were measured through the Tres Cruces Eastern Anticline. Site 8 corresponds to the eastern flank, site 9 to the western flank, and site 10 to the southwestward plunging anticlinal nose (Fig. 6). Four sets of sub-vertical tensile fractures were recognized in the area.

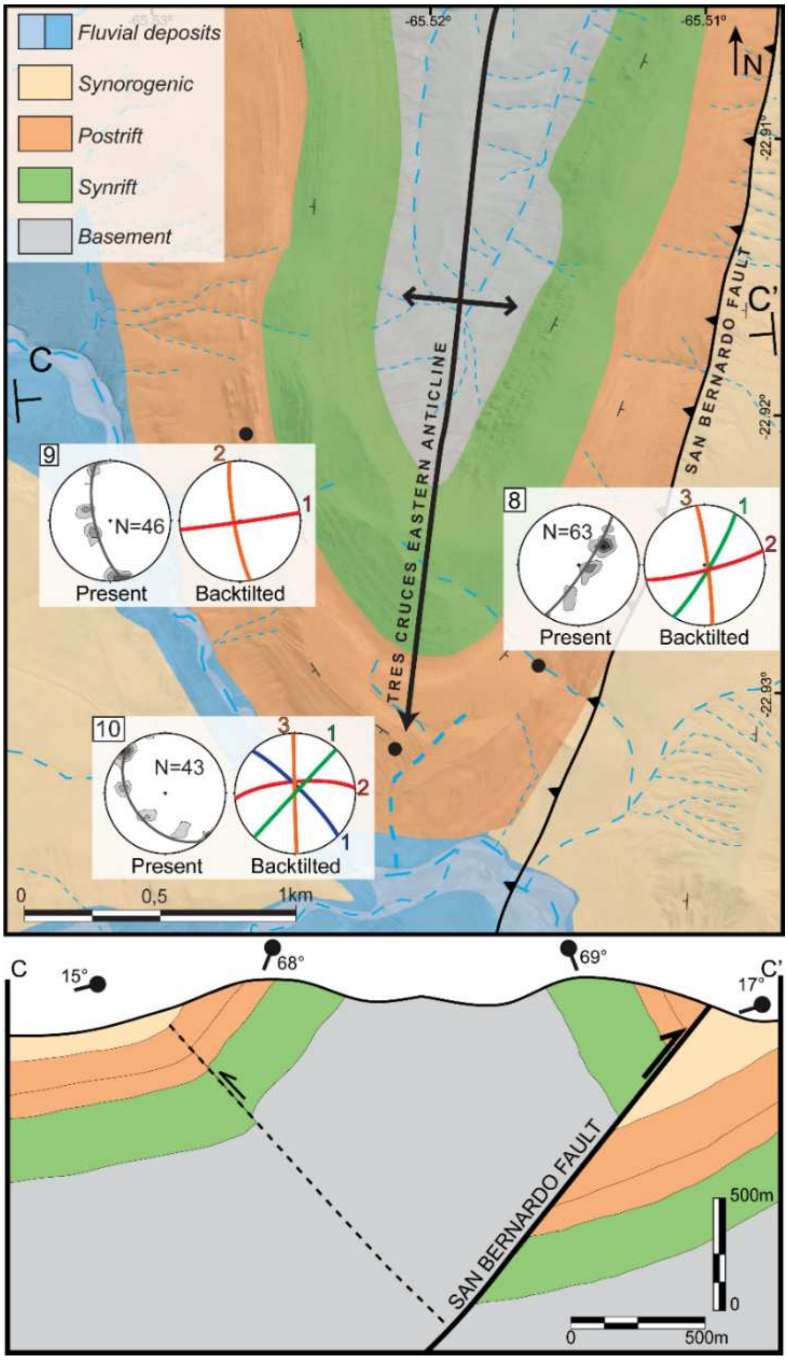

Fig. 6. Top: geological map of the Eastern Tres Cruces area (see Fig. 1 for structural references and location); black numbered dots indicate sampling sites. Equal-area plots show (left) present-day density contour of poles to planes and bed attitude (grey great circle), and (right) great circles for Fisher mean fracture set orientations in backtilted position. Numbers indicate the relative chronology observed, being 1 the oldest. Bottom: schematic cross-section, based on field data and proprietary 2D seismic lines (see location on map).

Sets ENE-WSW and N-S to NNW-SSE are present in all three sites (Figs. 6 and 7). On the one hand, set ENE-WSW is sub-perpendicular to the fold axis and shows great variability in terms of length, ranging from 50 cm to 1 m. On the other hand, fractures grouped in set N-S to NNW-SSE are shorter in length and they are sub-parallel to the fold axis.

The NE-SW trending set is well developed at sites 8 and 10; it is sub-parallel to the San Bernardo Fault (Fig. 6 and Fig. 7.d). Fracture traces lengths range from 60 cm to 2 meters. Finally, a minor set of NW-SE trending fractures was detected in site 10 (Fig. 7.d), with lengths exceeding the scanline diameter (2m).

Abutting relationships indicate that NW-SE and NE-SW sets are older than ENE-WSW set; N-S set is the youngest of the area (Fig. 7).

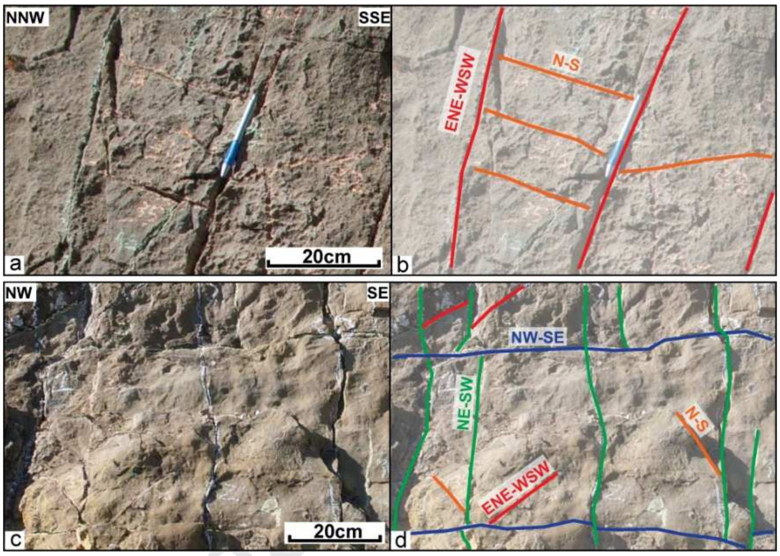

Fig. 7. Outcrop photographs and interpretation in site 9 (a and b) and in site 10 (c and d) showing examples of fracture patterns in the Eastern Tres Cruces area (see Fig. 6 for location).

4.4. Regional Pattern

Although considerable variations in fracture sets development can be identified between surveyed areas, a regional pattern can be clearly recognized. Comparative plots in Fig. 8 discriminate regional from local patterns. The sets that are compatible in terms of strike and chronology are denoted according to the set color code presented in previous figures. Numbers indicate relative chronology of occurrence only for those sets whose abutting relationships are well recognized and systematic.

NW-SE, NE-SW and ENE-WSW trending sets are present in the three working areas (Fig. 8). NW-SE set ranges from Az130° to Az150°. Fracture traces are long (more than 2 m) and they seem to be the oldest based on the abutting relationships (Figs. 3, 5 and 7). This set is subparallel to the NW-SE regional lineaments that control the structural setting of the area (Fig. 1).

An ENE-WSW set stands out in Fig. 8. These fractures are shorter and younger than the NW-SE and NE-SW fracture sets.

NE-SW set has variations between the three areas (Fig. 8). It is the most representative set in Arroyo Cóndor and is a minor set in San Bernardo and Eastern Tres Cruces area.

Moreover, in the San Bernardo area, this set seems to be younger than set NW-SE (Fig. 3.b and d), and it is coetaneous in the other two areas (Figs. 5 and 7).

The other recognized sets are unevenly distributed in the study area (Fig. 8). For example, although N-S to NNW-SSE set is not significant in the Arroyo Cóndor area, it is observed at San Bernardo and Eastern Tres Cruces area (Fig. 8), being the youngest set according to the abutting relationships. Finally, the WNW-ESE set is well defined only in the San Bernardo area (Figs. 2, 3 and 8).

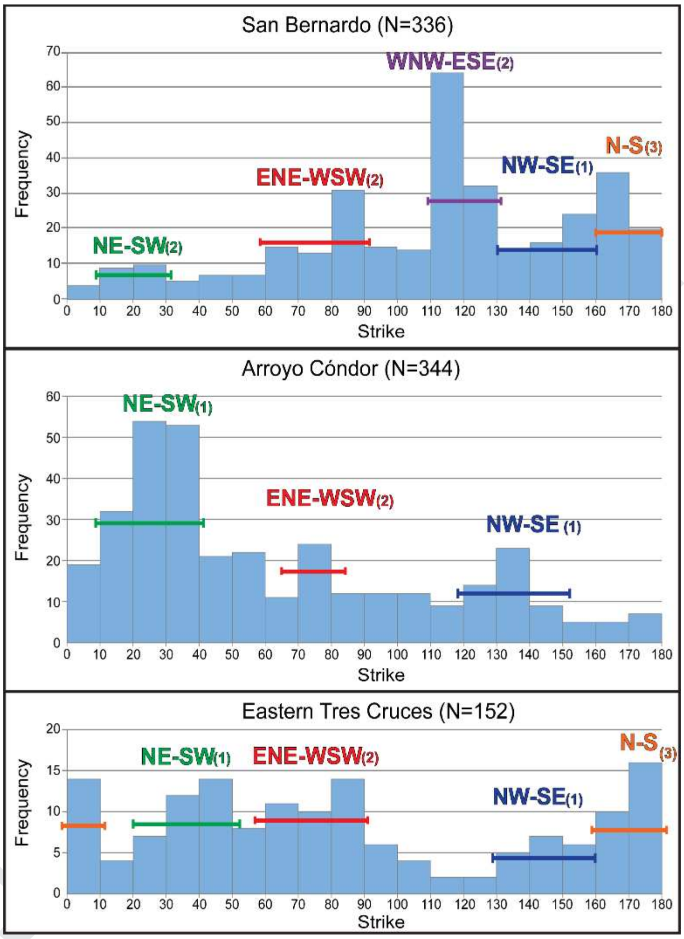

Fig. 8. Histograms showing fracture frequency versus strike for each study area: San Bernardo, Arroyo Cóndor and Eastern Tres Cruces. The fracture sets are indicated with colored bars, using the color code of previous figures. The relative chronology for each area is indicated with numbers, being 1 the oldest.

5. Discussion

In this section, the fracture framework presented above and their relative chronology are analyzed and framed within the Tres Cruces sub-basin structural and geodynamic evolution. A regional interpretation of the various fracture sets found is provided considering single-stage stress with local perturbations, which would have taken place during the Neogene. As it was mentioned in the tectonic setting section, this deformation stage, known as the Quechua phase, resulted in the main pulse of tectonic inversion of the Salta Rift Basin. According to paleomagnetic studies, an ENE-WSW directed convergence of the Nazca Plate towards South America has been acting in the studied Andean segment since that time (Pardo-Casas and Molnar, 1987; Somoza and Ghidella, 2012).

A 600 meters thick sequence of Casa Grande Formation is well exposed at the Tabladitas river, to the west of the Tabladitas village (Fig. 1.d). This sedimentary sequence is formed by red to reddish-brown siltstones and sandstones. The whole section has a homogeneous dip of ~40º W, without thickness variations of the strata. The absence of progressive unconformities or any other evidence of synsedimentary deformation suggests that this area was tectonically stable during the Eocene. 60 km south of this locality, Montero-López et al. (2018) recorded growth-strata in Casa Grande Formation along the western margin of the Sierra de Mal Paso, in the Eastern Cordillera. Considering stratigraphic and structural data from the southern parts of the Puna Plateau and the Eastern Cordillera, many authors agree in characterizing Eocene–Oligocene deformation as spatially disparate (Hongn et al., 2007; del Papa et al., 2013; Montero-López et al., 2018). This would have resulted in an undefined deformation front during that time. The highly fragmented and anisotropic crust overprinted by Paleozoic and Mesozoic tectonomagmatic processes would have influenced the disparate character of the thick-skinned deformation (e.g. Hongn et al., 2010; Montero-López et al., 2018). We propose that NW-SE lineaments of this area may have compartmentalized the deformation during the Paleogene. No evidence of early Cenozoic folding was recognized in the working areas, north of the Tres Cruces lineament, suggesting as a preliminary hypothesis that this NW-SE oriented lineament acted as a lateral ramp during the incipient Eocene deformation process, without any associate folding. Therefore, we consider that the main deformation stage and the consequent development of fracturing in our area occurred during the Neogene, under a stress field setting associated with the ENE-WSW convergence direction.

Several studies have shown that the presence of discontinuities can induce local perturbations of the stress field (Rawnsley et al., 1992; Homberg et al., 1997; Homberg et al., 2004; Maerten et al., 2016; Maerten et al., 2018). Based on numerical models, Homberg et al. (1997) analyzed the stress perturbation around a left-lateral strike-slip fault and described contractional and extensional zones for each fault tips. In contractional zones, stress trajectories are rotated in a clockwise sense (amount of rotation = β, Fig. 9.b I) disposing σ1 trajectories sub-parallel to the discontinuity, and in extensional zones, σ1 tend to become sub-perpendicular to the discontinuity as the rotation is in a counterclockwise sense (amount of rotation = α, Fig. 9.b I). During major fault zones reactivation, slip activity can occur along fault segments that induce the stress field deflections. Stress trajectories can adopt different perturbed directions as the active segment migrates along the fault zone, and then acquire the far-field orientation when the fault is inactive (Homberg et al., 1997; Homberg et al., 2004). Consequently, several local stress fields generated during a single tectonic event can be recognized adjacent to a major fault zone.

Four major long-lived structural lineaments (Tres Cruces, Ugchara, Tabladitas and Rumicruz; see Fig. 1.d) certainly controlled the structural setting of the study area. As stated above, these lineaments are interpreted as pre-Cretaceous basement heterogeneities, reactivated during the Cretaceous extensional phase. They are NW-SE trending subparallel structures, near which sub-meridian faults and folds develop sudden strike changes (Fig. 9.a). Taking the stress field perturbations model into account, it can be thus assumed that the presence of these first-order discontinuities might locally induce significant far-field stress perturbations. Consequently, σ1 trajectories would locally become sub-parallel or sub-perpendicular to the lineaments (represented in Fig. 9.b I).

The ENE-WSW Neogene convergence direction and the associated remote stress field are compatible with left-lateral strike-slip reactivation along the inherited NW-SE lineaments. Fault kinematics analysis over these transverse structures is still lacking. However, other first-order structures of the basin with the same orientation, like the Clama-Olapacato-Toro lineament, have evidence of sinistral kinematics (Marrett and Strecker, 2000; Seggiaro et al., 2016; García et al.,2019). Furthermore, left-lateral strike-slip reactivation has been reproduced in laboratory analogue models during an oblique contraction configuration (e.g. Yagupsky et al., 2008). Considering this context, a left-lateral sense of shear is expected to occur associated with the NW-SE oriented lineaments of the present study.

The identified tensile fracture sets can be used to indicate paleostress orientations, since their mean strike is perpendicular to the paleo-σ3 axis (Engelder, 1987). Therefore, it can be suggested that the NW-SE set was generated under a clockwise-rotated stress field, being the σ1 trajectories sub-parallel to the lineaments. The NE-SW fracture set is sub-perpendicular to the lineaments, and it could be responding to a counterclockwise-rotated stress field (Fig. 9.b I). Both sets are usually the oldest and they are identified in the three study areas. Some degree of dispersion between sites was found, whose origin would require further analysis. The collected data suggest that the first order lineaments were active during the formation of these fracture sets. This hypothesis is in good agreement with theoretical models in which under an active fault system, the orientation of natural fractures is influenced by the regional tectonic stress as well as by the perturbation of that stress state by nearby active larger faults (Peacock, 2001; Maerten et al., 2016).

South of the study area (>250 km), in the Calchaquí Valley, near the southern border of the Salta-Jujuy High (Fig. 1b), Hernandez and Franzese (2017) identified two sets of joints in the Yacoraite Formation outcrops. The oldest pattern they found consists of ENE-WSW to ESE-WNW and NNW-SSE- to NNE-SSW striking (cross) joints. The authors interpreted the occurrence of this joints pattern as the result of along-strike stretching of the Eocene foredeep zone of the thrust belt-foreland basin system (Quintà and Tavani, 2012; Tavani et al., 2015 and references therein). It is hard to reconcile the along-foredeep stretching hypothesis in our study area because it would require a NW-SE paleo-deformation front at the Tres Cruces sub-basin region during the early stages of Andean folding and thrusting. We consider that a better knowledge of the paleo-orogenic front geometry in the northern part of the Salta Rift Basin is needed to sustain this hypothesis. In addition, different strikes for this older joint pattern were found in both areas, meaning that the proposed hypothesis of a local perturbation of the ~ENE-WSW regional contraction (convergence direction during the Neogene) is more consistent in the area of this work.

The ENE-WSW set is parallel to the Neogene plate convergence direction. This set is well represented in all the working areas and it is usually younger than NW-SE and NE-SW sets. A reliable explanation for this relative chronology would be that the stress field adopts the far-field orientation (Fig. 9.b II) after successive periods of stress perturbation during the active stage of the lineaments. During this stage, the lineaments would have remained inactive, in coincidence with the migration of the active structures towards the foreland, reaching the southern Subandean wedge front (e.g., Echavarria et al., 2003; Brooks et al., 2011; Uba et al., 2009). Distinct phases of widening and thickening of the orogenic wedge via internal deformation are expected during this stage, as analogue and numerical models have shown (Adam et al., 2005; Del Castello and Cooke, 2007; Hoth et al., 2007; Yagupsky et al., 2014).

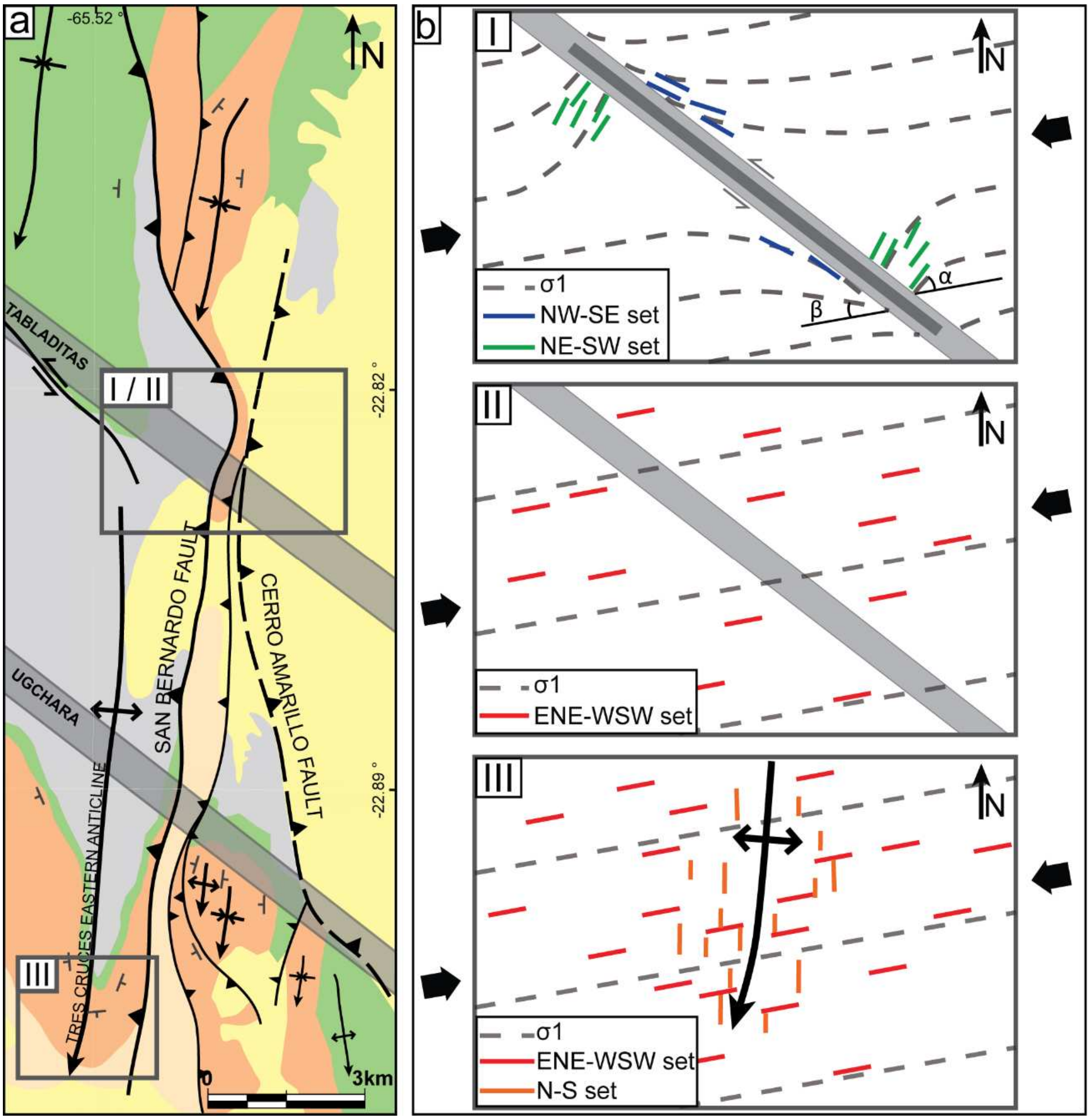

Fig. 9. a) Sector of the geological map of Fig. 1. Grey rectangles indicate the approximate location of the proposed conceptual models in (b). b) Conceptual models of the stress trajectories (based on Homberg et al., 2004) and fracture formation stages in the area during Neogene times. ENE-WSW convergence direction (black arrows) imposes the far-field stress. Regional lineaments are depicted with grey stripes and the stress trajectories in grey dashed lines. I) NW-SE and NE-SW fracture sets were formed during a period of stress field perturbation associated with the reactivation of segments (dark grey line) of the NW-SE regional lineaments (α and β are the amounts of counterclockwise and clockwise stress rotations). II) ENE-WSW fractures were formed parallel to the Neogene plate convergence direction (Somoza and Ghidella, 2012). III) N-S to NNW-SSE set were formed during folding sub-parallel to the fold axis.

Given that WNW-ESE fractures are only significant at the San Bernardo area (Fig. 8), they could be responding to local structural features. Proper analysis of the origin of this specific set deserves further study.

Finally, the N-S to NNW-SSE trending set is sub-parallel to the fold axes (Fig. 9.b III). It is generally the last one to be generated and fracture orientations are not affected after backtilting, as they are sub-parallel to the bedding strike. Therefore, the fractures were probably formed during a synfolding stage, when the folds started to grow (Stearns and Friedman, 1972; Twiss and Moores, 1973).

6. Conclusions

We present a fracture study of the Yacoraite Formation limestones in the Tres Cruces sub-basin, the northern depocenter of the Salta Rift Basin in Northwestern Argentina. Fracture attributes were measured over three folded structures: the San Bernardo Syncline, the Arroyo Cóndor folds and the Tres Cruces Eastern Anticline. Five joint sets oriented NW-SE, NE-SW, ENE-WSW, WNW-ESE and N-S to NNW-SSE were identified; the first four are likely to be prefolding, whereas the last one is classified as synfolding. Considering their orientation, distribution and abutting relationships, we propose a regional interpretation for the recognized settings. However, the lack of a concluding chronology must be considered and further studies are needed to improve the analysis of the fracture sets timing based on complementary techniques such as fillings analysis in thin sections.

We propose that single-stage stress far-field, directed ENE-WSW and active since the Neogene, can explain de recognized joint pattern. NW-SE and NE-SW sets would be related to perturbations of this same stress field, caused by pre-existing first-order anisotropies in the area (Tabladitas and Ugchara lineaments). Set ENE-WSW is compatible with the convergence direction acting since Neogene times. The WNW-ESE set origin remains unclear, it can be composed of joints related to a local structural feature. Finally, the N-S to NNW-SSE set is interpreted as a synfolding set associated with the beginning of the development of the studied folds.

These results provide the first comprehensive assessment of the natural fracture configuration of the Yacoraite Formation in the Tres Cruces sub-basin, related to the Neogene stress field which is controlled in turn by the large-scale boundary conditions (plate convergence). The perturbation of this far-field, associated with active stages of NW-SE lineaments, is invoked to explain the described setting.

The presence of basement anisotropies should be considered in fracture analysis since they can produce significant stress-field perturbations and control the fracture pattern development. Their effects need to be assessed to understand naturally fractured reservoirs such as the Yacoraite Formation.

Acknowledgments

This study has been supported by Agencia Nacional de Promoción Científica (PICT 2013-1309). We acknowledge Pablo Torres Carbonell, Fernando Hongn, anonymous reviewers and the editor Andrés Folguera for their valuable suggestions and constructive reviews. We also like to thank Paula Fernández Geyer for improving the English.

References

Adam, J., Urai, J. L., Wieneke, B., Oncken, O., Pfeiffer, K., Kukowski, N., Lohrmann, J., Hoth, S., van der Zee, W., Schmatz, J., 2005. Shear localization and strain distribution during tectonic faulting—New insights from granular-flow experiments and high-resolution optical image correlation techniques. Journal of Structural Geology 27(2), 283–301, doi:10.1016/j.jsg.2004.08.008.

Allmendinger, R. W., Cardozo, N., Fisher, D. M., 2012. Structural geology algorithms: Vectors and tensors. Cambridge University Press.

Allmendinger, R.W., Jordan, T.E., Kay, S.M., Isacks, B.L., 1997. The evolution of the Altiplano-Puna plateau of the Central Andes. Annual Review of Earth and Planetary Sciences 25(1), 139–174. https://doi.org/10.1146/annurev.earth.25.1.139

Bellahsen, N., Fiore Allwardt, P., Pollard, D.D., 2006. The role of fractures in the structural interpretation of Sheep Mountain Anticline, Wyoming. Journal of Structural Geology 28(5), 850–867. https://doi.org/10.1016/j.jsg.2006.01.013

Bergbauer, S., Pollard, D.D., 2004. A new conceptual fold-fracture model including prefolding joints, based on the Emigrant Gap anticline, Wyoming. Bulletin of the Geological Society of America 116(3-4), 294–307. https://doi.org/10.1130/B25225.1

Boll, A., Hernández, R.M., 1986. Interpretación estructural del área de Tres Cruces. Boletín de Informaciones Petroleras. Tercera Epoca 3(7), 2–14.

Bond, M., López, G., 1995. Los mamíferos de la Formación Casa Grande (Eoceno) de la provincia de Jujuy. Argentina. Ameghiniana 32(3), 301–309.

Brooks, B. A., Bevis, M., Whipple, K., Arrowsmith, J. R., Foster, J., Zapata, T., Kendrick, E., Minaya, E., Echalar, A., Blanco, A., Euillades, P., Sandoval, M., and Smalley Jr, R.J., 2011. Orogenic-wedge deformation and potential for great earthquakes in the central Andean backarc. Nature Geoscience 4, 380–383

Cardozo, N., Allmendinger, R.W., 2013. Spherical projections with OSXStereonet. Computers and Geosciences 51, 193–205. https://doi.org/10.1016/j.cageo.2012.07.021

Carrera, N., Muñoz, J.A., 2008. Thrusting evolution in the southern Cordillera Oriental (northern Argentine Andes): Constraints from growth strata. Tectonophysics 459(1-4), 107–122. https://doi.org/10.1016/j.tecto.2007.11.068

Carrera, N., Muñoz, J.A., Sàbat, F., Mon, R., Roca, E., 2006. The role of inversion tectonics in the structure of the Cordillera Oriental (NW Argentinean Andes). Journal of Structural Geology 28(11), 1921–1932. https://doi.org/10.1016/j.jsg.2006.07.006

Casini, G., Hunt, D.W., Monsen, E., Bounaim, A., 2016. Fracture characterization and modeling from virtual outcrops. AAPG Bulletin 100(1), 41–61. https://doi.org/10.1306/09141514228

Cladouhos, T.T., Allmendinger, R.W., Coira, B., Farrar, E., 1994. Late cenozoic deformation in the Central Andes: fault kinematics from the northern Puna, northwestern Argentina and southwestern Bolivia. Journal of South American Earth Sciences 7, 209–228. https://doi.org/10.1016/0895-9811(94)90008-6

Coutand, I., Cobbold, P.R., Urreiztieta, M. De, Gautier, P., Chauvin, A., Gapais, D., Rossello, A., De Urreiztieta, M., Gautier, P., Chauvin, A., Gapais, D., Rossello, E.A., López-Gamundí, O., 2001. Style and history of Andean deformation, Puna plateau, northwestern Argentina. Tectonics 20(2), 210–234. https://doi.org/10.1029/2000TC900031

Del Castello, M., Cooke, M. L., 2007. Underthrusting-accretion cycle: Work budget as revealed by the boundary element method. Journal of Geophysical Research, 112(B12), doi:10.1029/2007JB004997.

del Papa, C.E., Hongn, F.D., Petrinovic, I.A., Domínguez, R., 2004. Evidencias de deformación pre-miocena media asociada al antepaís andino en la Cordillera Oriental (24°35´ S - 66°12´ O). Revista de La Asociación Geológica Argentina 59(3), 506–509.

del Papa, C., Hongn, F., Powell, J., Payrola, P., Do Campo, M., Strecker, M.R., Petrinovic, I., Schmitt, A.K., Pereyra, R., 2013. Middle Eocene-Oligocene broken-foreland evolution in the Andean Calchaqui Valley, NW Argentina: Insights from stratigraphic, structural and provenance studies. Basin Research 25(5), 574–593. https://doi.org/10.1111/bre.12018

Disalvo, A., Rodríguez Schelotto, M., Gómez Omil, R., Hoffman, C., Benítez, J., Hurtado, S., 2002. Los reservorios de la Formación Yacoraite. In Schiuma, M., Hinterwimmer, G. y Vergani, G. (Eds.), Rocas Reservorio de Las Cuencas Productivas de La Argentina. V Congreso de Exploración y Desarrollo de Hidrocarburos, Mar Del Plata, 717–738.

Echavarria, L., Hernandez, R., Allmendinger, R., Reynolds, J., 2003. Subandean thrust and fold belt of northwestern Argentina: Geometry and timing of the Andean evolution. AAPG bulletin 87(6), 965-985.

Elger, K., Oncken, O., Glodny, J., 2005. Plateau-style accumulation of deformation: Southern Altiplano. Tectonics 24(4). https://doi.org/10.1029/2004TC001675

Engelder, T., 1987. Joints and shear fractures in rock. Fracture Mechanics of Rock 27–69.

Engelder, T., Lash, G.G., Uzcátegui, R.S., 2009. Joint sets that enhance production from Middle and Upper Devonian gas shales of the Appalachian Basin. AAPG Bulletin 93(7), 857–889. https://doi.org/10.1306/03230908032

Fisher, N.I., Lewis, T.L., and Embleton, B.J., 1987, Statistical analysis of spherical data: Cambridge, Cambridge University Press.

Gangui, A., Götze, H.J., 1996. The deep structure of the northern Puna, Argentina—constraints from 2D seismic data and 3D gravity modeling. XIII Congreso Geológico Argentino y III Congreso de Exploración de Hidrocarburos. Actas II, Buenos Aires, 545–565.

Gangui, A.H., 1998. A combined structural interpretation based on seismic data and 3-D gravity modeling in the Northern Puna/Eastern Cordillera, Argentina. Selbstverlag Fachbereich Geowissenschaften, FU Berlin.

García, V.H., Hongn, F., Yagupsky, D., Pingel, H., Kinnaird, T., Winocur, D., Cristallini, E., Robinson, R.A.J., Strecker, M.R., 2019. Late Quaternary tectonics controlled by fault reactivation. Insights from a local transpressional system in the intermontane Lerma valley, Cordillera Oriental, NW Argentina. Journal of Structural Geology 128, 103875. https://doi.org/10.1016/j.jsg.2019.103875

González, M.A., González, O.E., Pereya, F., Ramallo, E., Tchilinguirian, P., 2004. Hoja geológica 2366-IV, Ciudad del Libertador General San Martín. Programa Nacional de Cartas Geológicas de la República Argentina 1:250.000. SEGEMAR, Buenos Aires. Boletín 274.

Grier, M.E., Salfity, J.A., Allmendinger, R.W., 1991. Andean reactivation of the Cretaceous Salta rift, northwestern Argentina. Journal of South American Earth Sciences 4(4), 351–372.

Grosso, S., López, R., Vergani, G., O'leary, S., Lopez, R., Vergani, G., O'leary, S., 2013. Reservorios carbonáticos naturalmente fracturados en el Yacimiento Caimancito (Formación Yacoraite), cuenca cretácica del noroeste Argentino. Revista de La Asociación Geológica Argentina 70(1), 53–69.

Hancock, P.L.L., 1985. Brittle microtectonics: principles and practice. Journal of Structural Geology 7(3-4), 437–457. https://doi.org/10.1016/0191-8141(85)90048-3

Hardebol, N.J., Maier, C., Nick, H., Geiger, S., Bertotti, G., Boro, H., 2015. Multiscale fracture network characterization and impact on flow: A case study on the Latemar carbonate platform. Journal of Geophysical Research: Solid Earth 120(12), 8197–8222. https://doi.org/10.1002/2015JB011879.Received

Hernández, M., Franzese, J.R., 2017. The fracture patterns of the Tin Tin anticline: Fracturing process during the foreland evolution in the Calchaquí Valley, northwestern Argentina. Journal of Structural Geology 96, 54–64. https://doi.org/10.1016/j.jsg.2017.01.011

Hernández, M., Franzese, J.R., Vergani, G.D., 2016. Caracterización Estructural del Anticlinal Tin Tin: Aspectos Sobre su Estilo de Deformación y su Relación con la

Tectónica Cenozoica del Valle Calchaquí, Provincia de Salta. Revista de La Asociacion Geologica Argentina 73(3), 405–420.

Hernández, R.M., Disalvo, A., Boll, A., Gómez Omil, R.J., Galli, C., 1999. Estratigrafía secuencial del Grupo Salta, con énfasis en las subcuencas de Metán-Alemanía, noroeste Argentino. In Geología Del Noroeste Argentino: Relatorio, XIV Congreso Geológico Argentino: Salta, Argentina, Asociación Geológica Argentina. 264–284.

Homberg, C., Angelier, J., Bergerat, F., Lacombe, O., 2004. Using stress deflections to identify slip events in fault systems. Earth and Planetary Science Letters 217(3-4), 409–424. https://doi.org/10.1016/S0012-821X(03)00586-7

Homberg, C., Hu, J.C., Angelier, J., Bergerat, F., Lacombe, O., 1997. Characterization of stress perturbations near major fault zones: insights from 2-D distinct-element numerical modelling and field studies (Jura mountains). Journal of Structural Geology 19(5), 703–718. https://doi.org/10.1016/S0191-8141(96)00104-6

Hongn, F., del Papa, C., Powell, J.E., Petrinovic, I., Mon, R., Deraco, V., 2007. Middle Eocene deformation and sedimentation in the Puna – Eastern Cordillera transition (23°–26°S): Control by preexisting heterogeneities on the pattern of initial Andean shortening. Geological Society of America 35(3), 271–274. https://doi.org/10.1130/G23189A.1

Hongn, F.D., Tubía, J.M., Aranguren, A., Vegas, N., Mon, R., Dunning, G.R., 2010. Magmatism coeval with lower Paleozoic shelf basins in NW-Argentina (Tastil batholith): Constraints on current stratigraphic and tectonic interpretations. Journal of South American Earth Sciences 29, 289–305. https://doi.org/10.1016/j.jsames.2009.07.008

Hoth, S., Adam, J., Kukowsi, N., Oncken, O., 2007. Influence of erosion on the kinematics of bivergent orogens: Results from scaled sandbox simulations, in Tectonics, Climate, and Landscape Evolution, edited by S. D. Willett et al., Geological Society of America Special Paper, 398, 201–225.

Kley, J., Rossello, E.A., Monaldi, C.R., Habighorst, B., 2005. Seismic and field evidence for selective inversion of Cretaceous normal faults, Salta rift, northwest Argentina. Tectonophysics 399(1-4), 155–172. https://doi.org/10.1016/j.tecto.2004.12.020

Lacombe, O., Bellahsen, N., Mouthereau, F., 2011. Fracture patterns in the Zagros Simply Folded Belt (Fars, Iran): constraints on early collisional tectonic history and role of basement faults. Geological Magazine 148(5-6), 940–963. https://doi.org/10.1017/S001675681100029X

Maerten, L., Maerten, F., Lejri, M., 2018. Along fault friction and fluid pressure effects on the spatial distribution of fault-related fractures. Journal of Structural Geology 108, 198–212. https://doi.org/10.1016/j.jsg.2017.10.008

Maerten, L., Maerten, F., Lejri, M., Gillespie, P., 2016. Geomechanical paleostress inversion using fracture data. Journal of Structural Geology 89, 197–213. https://doi.org/10.1016/j.jsg.2016.06.007

Marquillas, R.A., del Papa, C., Sabino, I.F., 2005. Sedimentary aspects and paleoenvironmental evolution of a rift basin: Salta Group (Cretaceous–Paleogene), northwestern Argentina. International Journal of Earth Sciences 94(1), 94–113. https://doi.org/10.1007/s00531-004-0443-2

Marrett, R., Strecker, M.R., 2000. Response of intracontinental deformation in the central Andes to late Cenozoic reorganization of South American Plate motions. Tectonics 19(3), 452–467. https://doi.org/10.1029/1999TC001102

Mauldon, M., Dunne, W.M., Rohrbaugh Jr., M.B., 2001. Circular scanlines and circular windows: new tools for characterizing the geometry of fracture traces. Journal of Structural Geology 23(2-3), 247–258.

Mon, R., Salfity, J.A., 1995. Tectonic Evolution of the Andes of Northern Argentina. AAPG Memoir 62, 269–283.

Monaldi, C.R., Kley, J., Salfity, J.A., 2008a. Estructura del rift cretácico de Tres Cruces, provincia de Jujuy. Relatorio Del XVII Congreso Geológico Argentino. Jujuy, 233–243.

Monaldi, C.R., Salfity, J.A., Kley, J., 2008b. Preserved extensional structures in an inverted Cretaceous rift basin, northwestern Argentina: Outcrop examples and implications for fault reactivation. Tectonics 27(1). https://doi.org/10.1029/2006TC001993

Montero-López, C., del Papa, C., Hongn, F., Strecker, M.R., Aramayo, A., 2018. Synsedimentary broken-foreland tectonics during the Paleogene in the Andes of NW Argentine: new evidence from regional to centimetre-scale deformation features. Basin Research 30, 142–159. https://doi.org/10.1111/bre.12212

Moreno, J.A., 1970. Estratigrafía y paleogeografía del Cretácico Superior en la cuenca del noroeste argentino, con especial mención de los Subgrupos Balbuena y Santa Bárbara. Imprenta Coni SACIFI.

Nelson, R.A., 2001. Geologic analysis of naturally fractured reservoirs. Second ed. Woburn, Gulf Professional Publishing, 332.

Oncken, O., Hindle, D., Kley, J., Elger, K., Victor, P., Schemmann, K., 2006. Deformation of the Central Andean Upper Plate System – Facts, Fiction, and Constraints for Plateau Models. In The Andes: Active Subduction Orogeny, 3–27. Springer, Berlin.

Panza, E., Agosta, F., Rustichelli, A., Zambrano, M., Tondi, E., Prosser, G., Giorgioni, M., Janiseck, J.M., 2016. Fracture stratigraphy and fluid flow properties of shallow-water, tight carbonates: The case study of the Murge Plateau (southern Italy). Marine and Petroleum Geology 73, 350–370. https://doi.org/10.1016/j.marpetgeo.2016.03.022

Pardo-Casas, F., Molnar, P., 1987. Relative motion of the Nazca (farallon) and South American plates since late Cretaceous time. Tectonics 6(3), 233–248.

Payrola Bosio, P., Powell, J., del Papa, C., Hongn, F., 2009. Middle Eocene deformation-sedimentation in the Luracatao Valley: Tracking the beginning of the foreland basin of northwestern Argentina. Journal of South American Earth Sciences 28(2), 142–154. https://doi.org/10.1016/j.jsames.2009.06.002

Peacock, D.C.P., 2001. The temporal relationship between joints and faults. Journal of Structural Geology 23(2-3), 329-341.

Peacock, D.C.P., Sanderson, D.J., 2018. Structural analyses and fracture network characterisation: Seven pillars of wisdom. Earth-Science Reviews 184, 13–28. https://doi.org/10.1016/j.earscirev.2018.06.006

Pollard, D.D., Aydin, A., 1988. Progress in understanding jointing over the past century. Geological Society of America Bulletin 100(8), 1181–1204. https://doi.org/10.1130/0016-7606(1988)100<1181

Priest, S.D., Hudson, J.A., 1981. Estimation of discontinuity spacing and trace length using scanline surveys. International Journal of Rock Mechanics and Mining Sciences & Geomechanics Abstracts. Pergamon, 18(3), 183–197.

Quintà, A., Tavani, S., 2012. The foreland deformation in the south-western Basque-Cantabrian Belt (Spain). Tectonophysics 576–577, 4–19. https://doi.org/10.1016/j.tecto.2012.02.015

Rawnsley, K.D., Rives, T., Petit, J.P., Hencher, S.R., Lumsden, A.C., 1992. Joint development in perturbed stress fields near faults. Journal of Structural Geology 14(8-9), 939–951. https://doi.org/10.1016/0191-8141(92)90025-R

Reyes, F.C., 1972. Correlaciones en el Cretácico de la cuenca Andina de Bolivia, Perú y Chile. Revista Técnica de YPFB 1, 101–144.

Reyes, F.C., Salfity, J.A., 1973. Consideraciones sobre la estratigrafía del Cretácico (Subgrupo Pirgua) del noroeste argentino. In V Congreso Geológico Argentino: Buenos Aires, Argentina, Asociación Geológica Argentina. 355–385.

Rohrbaugh Jr., M.B., Dunne, W.M., Mauldon, M., 2002. Estimating fracture trace intensity, density, and mean length using circular scan lines and windows. AAPG Bulletin 86(12), 2089–2104.

Rubiolo, D., Seggiaro, R.E., Gallardo, E., Disalvo, A., Sánchez, M., Turel, A., Ramallo, E., Sandrus, A., Godeas, M., 2001. Hoja Geológica 2366-II/2166-IV, La Quiaca. Geología y Provincia de Jujuy y Salta. Servicio Geológico Minero Argentino. Boletín 246.

Salfity, J.A., Marquillas, R.A., 1994. Tectonic and sedimentary evolution of the Cretaceous-Eocene Salta Group basin, Argentina. In: Salfity, J.A. (Ed.), Cretaceous Tectonics of the Andes. Earth Evolution Sciences, Friedr. Vieweg and Sohn, 266–315.

Salfity, J.A., Marquillas, R.A., 2000. La cuenca cretácico-terciaria del norte argentino. Geología Argentina, Instituto Argentino de Geología y Recursos Minerales, Anales 29, 613–626.

Seggiaro, R., Guzmán, S., Pereyra, R., Coppolecchia, M., Cegarra, M., 2016. Neotectonics and quaternary monogenetic volcanism above the central segment of the calama olacapato toro lineament, NW argentina. Revista de la Asociación Geológica Argentina, 73(4), 468-477.

Somoza, R., Ghidella, M.E., 2012. Late Cretaceous to recent plate motions in western South America revisited. Earth and Planetary Science Letters 331, 152–163 https://doi.org/10.1016/j.epsl.2012.03.003

Starck, D., 2011. Cuenca Cretácica-Paleógena del Noroeste Argentino. In VIII Congreso de Exploración y Desarrollo de Hidrocarburos Simposio Cuencas Argentinas: Visión Actual, Instituto Argentino Del Petróleo y El Gas. 407–453.

Stearns, D.W., Friedman, M., 1972. Reservoirs in Fractured Rock. AAPG, Memoir 16, 82–106.

Tavani, S., Storti, F., Fernández, O., Muñoz, J.A., Salvini, F., 2006. 3-D deformation pattern analysis and evolution of the Añisclo anticline, southern Pyrenees. Journal of Structural Geology 28, 695–712. https://doi.org/10.1016/j.jsg.2006.01.009

Tavani, S., Storti, F., Lacombe, O., Corradetti, A., Muñoz, J.A., Mazzoli, S., 2015. A review of deformation pattern templates in foreland basin systems and fold-and-thrust belts: Implications for the state of stress in the frontal regions of thrust wedges. Earth-Science Reviews 141, 82–104. https://doi.org/10.1016/j.earscirev.2014.11.013

Twiss, R.J., Moores, E.M., 1973. Structural Geology. W.H. Freeman and Company, New York.

Uba, C., Kley, J., Strecker, M.R., Schmitt, A.K., 2009. Unsteady evolution of the Bolivian Subandean thrust belt: the role of enhanced erosion and clastic wedge progradation. Earth and Planetary Science Letter 281, 134–146.

Yagupsky, D., Brooks, B. A., Whipple, K. X., Duncan, C. C., Bevis, M., 2014. Distribution of active faulting along orogenic wedges: Minimum-work models and natural analogue. Journal of Structural Geology 66, 237–247.

Yagupsky, D.L., Cristallini, E., Fantín, J., Valcarce, G.Z., Bottesi, G., Varadé, R., 2008. Oblique half-graben inversion of the Mesozoic Neuquén Rift in the Malargüe Fold and Thrust Belt, Mendoza, Argentina: New insights from analogue models. Journal of Structural Geology 30, 839–853. https://doi.org/10.1016/j.jsg.2008.03.007

Highlights

- A fracture network analysis over the Yacoraite Formation limestones in the Tres Cruces sub-basin was performed.
- Five main fracture sets trending NW-SE, NE-SW, ENE-WSW, N-S and WNW-ESE were identified.
- A single-stage stress far-field is proposed to explain de recognized fracture pattern.
- Stress perturbations due to preexisting crustal anisotropies exert major control on fracture patterns.

Author Contribution Statement

Conceptualization: CCL and DY; *Methodology*: JL, DY and CCL; *Formal analysis*: CCL; *Investigation*: DY, JL and CCL, *Writing – Original draft*: CCL, DY and JL, *Visualization*: CCL, *Funding acquisition*: DY and JL

Declaration of interests

☒ The authors declare that they have no known competing financial interests or personal relationships that could have appeared to influence the work reported in this paper.

☐The authors declare the following financial interests/personal relationships which may be considered as potential competing interests: